

# Extraction of the species-dependent dipole amplitude and phase from high-order harmonic spectra in rare-gas atoms

Anh-Thu Le,<sup>1</sup> Toru Morishita,<sup>1,2</sup> and C. D. Lin<sup>1</sup>

<sup>1</sup>*Department of Physics, Cardwell Hall, Kansas State University, Manhattan, Kansas 66506, USA*

<sup>2</sup>*Department of Applied Physics and Chemistry, University of Electro-Communications, 1-5-1 Chofu-ga-oka, Chofu-shi, Tokyo, 182-8585, Japan*

*and PRESTO, Japan Science and Technology Agency, Kawaguchi, Saitama 332-0012, Japan*

(Received 20 December 2007; published 11 August 2008)

Based on high-order harmonic generation (HHG) spectra obtained from solving the time-dependent Schrödinger equation for atoms, we established quantitatively that the HHG yield can be expressed as the product of a returning electron wave packet and photorecombination cross sections, and the shape of the returning wave packet is shown to be largely independent of the species. By comparing the HHG spectra generated from different targets under identical laser pulses, accurate structural information, including the phase of the recombination amplitude, can be retrieved. This result opens up the possibility of studying the target structure of complex systems, including their time evolution, from the HHG spectra generated by short laser pulses.

DOI: [10.1103/PhysRevA.78.023814](https://doi.org/10.1103/PhysRevA.78.023814)

PACS number(s): 42.65.Ky, 31.70.Hq, 33.80.Rv, 42.30.Tz

## I. INTRODUCTION

When an atom is subjected to a strong driving laser field, one of the most important nonlinear response processes is the generation of high-order harmonics. In the past decade, high-order harmonic generation (HHG) has been used for the production of single attosecond pulses [1–3] and attosecond pulse trains [4], thus opening up new opportunities for attosecond time-resolved spectroscopy. HHG is understood using the three-step model (TSM) [5–7]—first, the electron is released by tunnel ionization; second, it is accelerated by the oscillating electric field of the laser and later driven back to the target ion; and third, the electron recombines with the ion to emit a high-energy photon. A semiclassical formulation of the TSM based on the strong-field approximation (SFA) is given by Lewenstein *et al.* [7]. In this model (often called the Lewenstein model), the liberated continuum electron experiences the full effect from the laser field, but not from the ion that it has left behind. In spite of this limitation, the SFA model has been used quite successfully, in particular, for analysis of the attosecond synchronization of high harmonics; see Mairesse *et al.* [8] and references therein. However, since the continuum electron recombines when it is near the parent ion, neglect of the electron-ion interaction in the SFA model is rather questionable.

Besides the SFA model, HHG can also be calculated by solving the time-dependent Schrödinger equation (TDSE) numerically. However, the latter has been mostly applied to atomic targets only and under the single active electron (SAE) approximation. For molecular targets, TDSE calculations are difficult to carry out. Thus to understand HHG from molecular targets, an alternative theoretical model which is more accurate than the SFA but computationally less demanding than the TDSE is highly desirable. In a recent paper [9] based on an extension of the three-step model, we have shown that accurate HHG yield can be expressed as

$$S(\omega) = W(E)|d(\omega)|^2, \quad (1)$$

where  $d(\omega)$  is the “exact” photorecombination (PR) transition dipole and  $W(E)$  describes the flux of returning electron,

which we will call a “wave packet.” The validity of this model has been tested on rare-gas atoms [9] and, more recently, on HHG from aligned  $\text{H}_2^+$  molecules [10].

The factorization, Eq. (1), was first proposed by Itatani *et al.* [11], except that they assumed that the dipole matrix element can be calculated by treating the continuum electrons as plane waves. Based on the latter approximation, they proposed the tomographic method for imaging the wave function of the highest occupied molecular orbital from the measured HHG. The limitation of approximating continuum electrons with plane waves, as well as the tomographic method, has been addressed previously by Le *et al.* [12].

Equation (1) above treats the intensity of the HHG yields only. In practice, the emitted harmonics also contain phase information. The phase of the high-order harmonics has been investigated in a number of papers, using different experimental methods [13–17] for unaligned or partially aligned molecules. Furthermore, in order to compare with experiments the macroscopic propagation effect has to be included. In this case, the phase of the harmonics generated by single atoms or molecules is also needed. In macroscopic propagation, high-order harmonics are generated from atoms or molecules within the interaction volume, which has different laser intensities. Thus in general HHG spectra have to be calculated over hundreds of intensities. This also points out the need of finding an easier way to calculate harmonics generated from single atoms or molecules.

In this paper, we have two goals. The first is to show that electron wave packets obtained from the SFA model and from the TDSE calculation are nearly identical, but the transition dipoles calculated from the plane-wave approximation (PWA) are significantly different from using scattering waves (SWs). This result suggests a scattering-wave-based strong-field approximation (SW-SFA) for harmonic generation where the wave packet is derived from the SFA, but the transition dipole is calculated using accurate SW. The second goal is to check whether Eq. (2) is indeed valid to the level of *complex* amplitudes such that one can relate the phases of

HHG to the phases in the transition dipoles. Since phases of harmonics can be measured [13–17] and they are needed in order to incorporate the effect of propagation in the macroscopic medium, such a study is important.

## II. MODEL AND THEORETICAL METHOD

In this paper we seek to generalize Eq. (1) in the form that the induced dipole  $D(\omega)$  can be written as

$$|D(\omega)|e^{i\phi} = |W(E)|^{1/2}e^{i\eta}|d(\omega)|e^{i\delta(\omega)}, \quad (2)$$

where  $\delta(\omega)$  and  $\eta(E)$  are the phase of the PR transition dipole and the wave packet, respectively. Electron energy  $E$  is related to the emitted photon energy  $\omega$  by  $E = \omega - I_p$ , with  $I_p$  being the ionization potential of the target. Clearly the HHG signal  $S(\omega) \sim \omega^4 |D(\omega)|^2$  and  $W(E)$  depend on the laser properties. On the other hand,  $d(\omega)$  is the property of the target only. The factorization in Eq. (1) is most useful when one compares the HHG spectra from two different targets in the identical laser field. Assuming that the shape of  $W(E)$  is species independent, by measuring the relative HHG yields, one can deduce the PR cross section of one species if the PR cross section of the other is known. As stated earlier, the validity of Eq. (2) on the level of *amplitudes* has been shown recently in Morishita *et al.* [9] using HHG spectra calculated by solving the TDSE for atoms. Indications for the validity of this factorization have also been shown for rare-gas atoms by Levesque *et al.* [18] and for  $N_2$  and  $O_2$  molecules [12], where the HHG spectra were calculated using the SFA model. In the SFA the continuum electron is approximated by plane waves; thus, the dipole matrix elements are calculated in the PWA.

Here we comment on the computational details. The solution of the TDSE and the choice of one-electron model potential for describing the atom have been described previously [19]. The electric field of the laser pulse is written in the form  $E(t) = E_0 a(t) \cos(\omega t)$ , with the envelope given by  $a(t) = \cos^2(\pi t / \tau)$ , where  $\tau$  is 2.75 times the full width at half maximum (FWHM) of the laser pulse. To calculate the PR cross section, the scattering wave function is expanded in terms of partial waves [20] and the transition dipole is calculated for the continuum electron that has the wave vector along the polarization axis only.

## III. RESULTS AND DISCUSSION

First in Fig. 1 we compare the PR cross sections of Ar, Xe, and Ne calculated by treating the continuum electrons using the PWA to results calculated with accurate SWs. Clearly they show significant differences. They reflect the well-known facts that plane waves are poor approximations for representing continuum electrons in atoms and molecules for energies in the energy range of tens to hundreds of eV.

Next we compare in Fig. 2 the wave packets  $W(E)$  for Ne deduced from the TDSE and SFA results using Eq. (1). In the SFA case, the transition dipole is calculated within the PWA. Also shown is the  $W(E)$  obtained from scaled atomic hydrogen, with the effective nuclear charge chosen such that the ionization potential of its  $1s$  ground state is the same as of

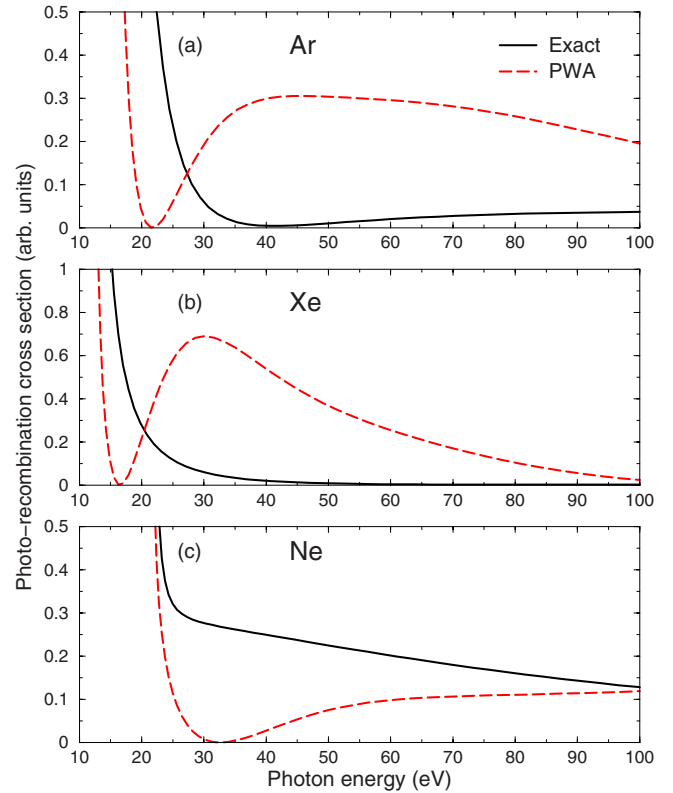


FIG. 1. (Color online) Photorecombination cross sections of Ar (a), Xe (b), and Ne (c), obtained by using exact scattering wave functions (solid black curves) and within the plane-wave approximation (dashed red curves) for the continuum electrons.

Ne( $2p$ ). We used a laser pulse with duration (FWHM) of 10.3 fs, peak intensity of  $2 \times 10^{14}$  W/cm<sup>2</sup>, and mean wavelength of 1064 nm. Note that we have normalized the results near the cutoff. The normalization is to account for the difference in the tunneling ionization rates from the SFA and

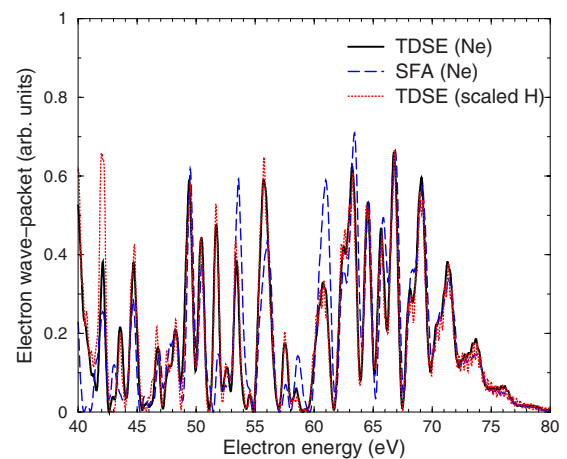


FIG. 2. (Color online) Comparison of the returning electron “wave packets” extracted from the HHG spectra of Ne, obtained by solving the TDSE (solid black line) and from the SFA model (dashed blue line). Also shown is the TDSE result for the wave packet from scaled H (dotted red line). For laser parameters, see text.

TDSE, or from the different species. This comparison shows that the shape, or the energy dependence, of the returning wave packets depends only on the laser parameters.

Having established that the wave packet can be obtained from the SFA model, we now examine the accuracy of HHG calculated using the SW-SFA model where the wave packet is extracted from the SFA model and the transition dipoles are calculated using SWs. In other words, the HHG yield is obtained by  $S^{SW-SFA}(\omega) = S^{SFA}(\omega) \left| \frac{d(\omega)}{d^{PWA}(\omega)} \right|^2$ . In Fig. 3 we show the HHG spectra obtained from the TDSE, SFA, and SW-SFA for Ar, Xe, and Ne. For Ar and Ne, the laser pulse has a peak intensity of  $2 \times 10^{14}$  W/cm<sup>2</sup> and mean wavelength of 800 nm. The laser duration (FWHM) is 10 fs for Ar and 20 fs for Ne. For Xe, the corresponding parameters are  $5 \times 10^{13}$  W/cm<sup>2</sup>, 1600 nm, and 7.8 fs, respectively. The HHG yields for Ar are shifted vertically in order to show their detailed structures. For Ne and Xe, the SFA and SW-SFA results are normalized to the TDSE results near the cutoff—i.e., close to  $3.2U_p + I_p$ , where  $U_p$  is the ponderomotive energy.

The results in Fig. 3 clearly demonstrate the good improvement of the SW-SFA over the SFA in achieving better agreement with the TDSE results. Here we use the TDSE results as benchmarks for the approximate theories. This makes sense as for each atomic target the same model potentials are used in both the TDSE and SW-SFA. Note that the position of the Cooper minimum seen in the HHG spectra for Ar near 40 eV [see Fig. 3(a), Fig. 4(a) below, and also Fig. 1(a)] is shifted compared to the photoionization experimental value of 47 eV. To fully reproduce experiments, one needs to account for the multielectron effect. This has been well understood; see, for example, [21,22].

Since the SFA gives the correct wave packet, its prediction would be “reasonable” in the energy region where the dipole matrix element is rather flat—i.e., in the higher photon energy region. Thus the SFA would give an adequate prediction of the HHG spectra usually near the cutoff region (after spectra are renormalized). This fact has been known [7]. The improvement of the SW-SFA occurs usually at lower photon energies where the PWA for the continuum electron is grossly incorrect. In particular, the transition dipole from PWA goes through zero at some lower energies; see Fig. 1. This is the energy region where the SFA suffers the largest errors. Because of the zeros in the dipole matrix elements in the PWA, the deduced wave packets from SFA would suffer large errors at the corresponding energies. These errors are reflected as the sharp spikes in the HHG spectra calculated using the SW-SFA model.

For a realistic description of the experimental harmonic spectra, the effect of phase matching and macroscopic propagation should be addressed. To this end, knowledge of the harmonic phase is necessary. First, we establish that there is a close relationship between the harmonics phase  $\phi$  and the PR dipole phase  $\delta$ . To be specific, we focus on Ar target. We calculated the phase difference  $\Delta\phi$  for each harmonic generated from Ar and from its scaled hydrogen (reference) partner under the same laser pulse. These calculations were carried out using the TDSE with four cycle and ten cycle laser pulses, intensities of 1 and  $2 \times 10^{14}$  W/cm<sup>2</sup>, and wavelengths of 1064 nm and 800 nm. In Fig. 4(a) we compare

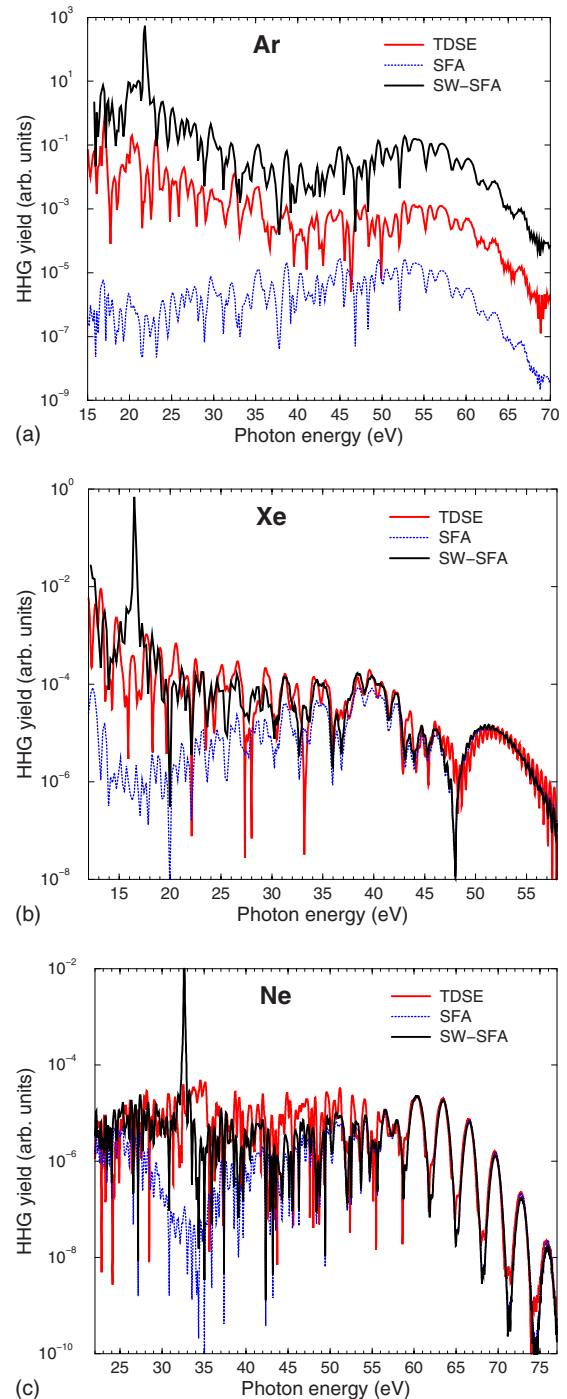


FIG. 3. (Color online) Comparison of the HHG yields obtained from numerical solution of the TDSE (solid red lines), the SFA (dotted blue lines), and the SW-SFA model (solid black lines) for Ar (a), Xe (b), and Ne (c). Data for Ar have been shifted vertically to show the detailed structures. For laser parameters, see text.

$\Delta\phi = \phi^{Ar} - \phi^{ref}$  with the PR dipole phase difference  $\Delta\delta = \delta^{Ar} - \delta^{ref}$ . Here we have shifted the harmonic phase difference to match the PR dipole phase difference at  $E=60$  eV. Clearly, the two agree very well for the different lasers used. In particular, the phase jump near 40 eV (due to the Cooper minimum in Ar) is well reproduced. This indicates that the phases of the wave packets from the two sys-

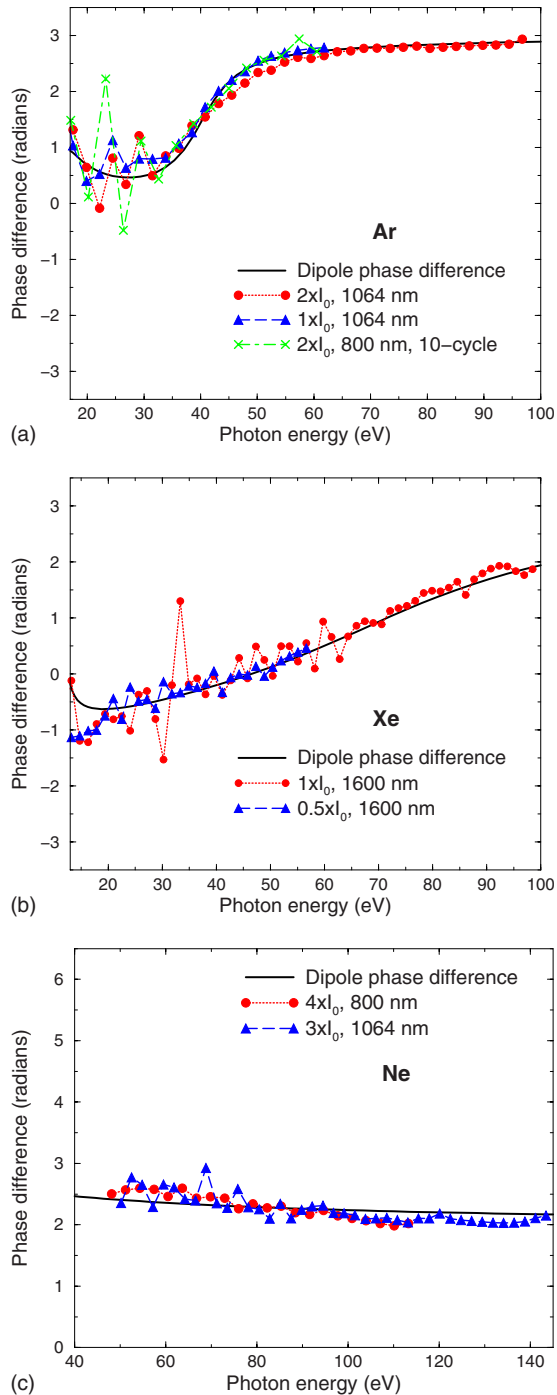


FIG. 4. (Color online) Extracted harmonic phase difference  $\Delta\phi$  between Ar and scaled hydrogen obtained with different lasers as function of emitted photon energy. The PR dipole phase difference  $\Delta\delta$  is given as solid black line. (a) Ar, (b) Xe, and (c) Ne.  $I_0 = 10^{14}$  W/cm<sup>2</sup>.

tems are almost identical (up to a constant shift). Similar agreements were also found for Xe and Ne, as shown in Figs. 4(b) and 4(c), respectively. Here laser pulses of four cycles duration are used; other parameters are given as shown in the labels. This result allows one to obtain the harmonic phase  $\phi$  from the harmonic phase of the partner atom  $\phi^{ref}$  by using  $\phi = \phi^{ref} + \Delta\delta$ .

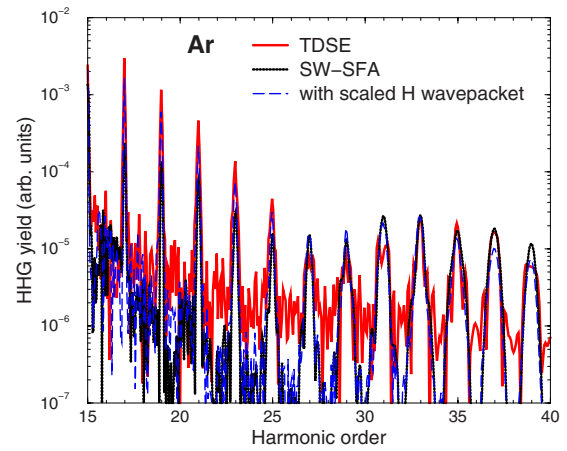


FIG. 5. (Color online) HHG spectra for Ar from the “simulated” macroscopic propagation. Shown are results from the exact TDSE (solid red line) and SW-SFA (dotted black line), and by using the wave packet extracted from TDSE solution for scaled H(1s) (dashed blue line). For laser parameters, see text.

We have also applied the same procedure by comparing the TDSE and SFA results for the same target and found that  $\Delta\tilde{\phi} = \phi^{TDSE} - \phi^{SFA}$  no longer agrees well with  $\Delta\tilde{\delta} = \delta^{SW} - \delta^{PW}$ . This indicates that the phase of the electron wave packet calculated from the SFA differs from the one calculated by the TDSE, although their magnitudes agree reasonably well. How significantly do these differences affect the HHG spectra after macroscopic propagation? To this end we calculate the HHG spectra by coherently averaging the induced polarization over an intensity range of the driving laser. In Fig. 5 we show the results for Ar from the TDSE, the SW SFA, and the one with the wave packet extracted from the scaled hydrogen. All of these results are coherently averaged over 11 equally spaced intensities in the range from  $1.8$  to  $2.2 \times 10^{14}$  W/cm<sup>2</sup>. The laser is of 800 nm wavelength and 30 fs (FWHM). The scaled H result is indeed in quite good agreement with the exact TDSE calculations. This is not surprising since we have shown that the phases of the wave packet from the scaled H and from Ar are almost identical at a single intensity. For the SW-SFA, the agreement is not as good, but the improvement over the SFA is still significant. The phase in the SFA (or the SW-SFA) can probably be improved by adding some correction to the semiclassical action, for example, as has been suggested in [23,24]. At present, it is better to extract the phase of the wave packet from the companion atomic target where TDSE calculations can be carried out.

Before concluding, we mention several earlier related works. There exists a wealth of literature aiming at improving the SFA model, e.g., by including Coulomb distortion [23,25], or by eikonal approximations [24]. In these approaches, the PR processes are still treated approximately. For example, use of Coulomb wave for the continuum electron would not produce the Cooper minimum in the PR cross section in Ar (see Fig. 1). The advantage of the SW-SFA is that it factors out the target structure explicitly. A minimum in the HHG spectra may be attributed to the minimum in the PR cross section, and this position should not change with

laser parameters. Such minima are of particular interest for molecular targets since minima in the molecular dipole matrix element may be interpreted as due to the interference between the emission amplitudes from different atomic centers. Interference minima have been observed experimentally in CO<sub>2</sub> by different groups [26,27], but the observed positions of the minimum are not identical and thus other possible interpretations have been suggested [28]. Another hot topic in recent years is the tomographic method for imaging the molecular orbitals [11]. This pioneering work deduced the dipole matrix elements of N<sub>2</sub> molecules by comparing the HHG spectra of N<sub>2</sub> vs Ar using the factorization, Eq. (1), but with both dipoles being treated within the PWA. Furthermore, we note that in Ref. [11], the continuum electron energy is set equal to the photon energy, arguing that the electron recombining near the core should gain the additional binding energy. For Ar, this would shift the PWA curve in Fig. 1 by 15.7 eV, making the PWA result much closer to the SW result. However, this shift does not always work; see the Xe and Ne examples in Fig. 1.

#### IV. SUMMARY AND CONCLUSIONS

In conclusion, we have established quantitatively that the last step of the three-step model of HHG can indeed be expressed as the photorecombination process of the returning electron wave packet. The wave packet depends nonlinearly

on the laser, but its shape and phase are largely independent of the target. Thus, if the PR of a reference target is known, the PR of another target can be derived by measuring the HHG of the two species under identical laser pulses. Since the results should be independent of the lasers, this allows for an important check on the accuracy of the measurements. We also showed that the HHG spectra can be calculated using the SW-SFA model. This model describes well the single-atom HHG intensity, but the phase needs further corrections. For complex systems, the SW-SFA would be a good starting point for describing the HHG spectra since the PR process is accurately incorporated. While our conclusion has been derived based on atomic targets and in the single-active-electron model, we anticipate that the results are applicable to molecules where accurate TDSE calculations are not available in general. The present result offers a systematic roadmap for extracting target structure information from the high-order harmonics generated by intense lasers.

#### ACKNOWLEDGMENTS

This work was supported in part by the Chemical Sciences, Geosciences and Biosciences Division, Office of Basic Energy Sciences, Office of Science, (U.S.) Department of Energy. T.M. is also supported by a Grant-in-Aid for Scientific Research (C) from MEXT, Japan, by the 21st Century COE program on “Coherent Optical Science,” and by a JSPS Bilateral joint program between the U.S. and Japan.

- 
- [1] M. Drescher, M. Hentschel, R. Kienberger, M. Uiberacker, V. Yakovlev, A. Scrinizi, T. Westerwalbesloh, U. Kleineberg, U. Heinzmann, and F. Krausz, *Nature (London)* **419**, 803 (2002).
- [2] T. Sekikawa, A. Kosuge, T. Kanai, and S. Watanabe, *Nature (London)* **432**, 605 (2004).
- [3] G. Sansone, E. Benedetti, F. Calegari, C. Vozzi, L. Avaldi, R. Flammini, L. Poletto, P. Villoresi, C. Altucci, R. Velotta, S. Stagira, S. De Silvestri, and M. Nisoli, *Science* **314**, 443 (2006).
- [4] R. Lopez-Martens, K. Varju, P. Johnsson, J. Mauritsson, Y. Mairesse, P. Salieres, M. B. Gaarde, K. J. Schafer, A. Persson, S. Svanberg, C.-G. Wahlstrom, and A. L’Huillier, *Phys. Rev. Lett.* **94**, 033001 (2005).
- [5] P. B. Corkum, *Phys. Rev. Lett.* **71**, 1994 (1993).
- [6] K. C. Kulander, K. J. Schafer, and J. L. Krause, in *Super Intense Laser-Atom Physics*, Vol. 316 of *NATO Advanced Study Institute, Series B: Physics*, edited by B. Piroux (Plenum, New York, 1993), p. 95.
- [7] M. Lewenstein, Ph. Balcou, M. Yu. Ivanov, A. L’Huillier, and P. B. Corkum, *Phys. Rev. A* **49**, 2117 (1994).
- [8] Y. Mairesse, A. de Bohan, L. J. Frasinski, H. Merdji, L. C. Dinu, P. Monchicourt, P. Breger, M. Kovacev, R. Taieb, B. Carre, H. G. Muller, P. Agostini, and P. Salieres, *Science* **302**, 1540 (2003).
- [9] T. Morishita, A. T. Le, Z. Chen, and C. D. Lin, *Phys. Rev. Lett.* **100**, 013903 (2008).
- [10] A. T. Le, R. D. Picca, P. D. Fainstein, D. A. Telnov, M. Lein, and C. D. Lin, *J. Phys. B* **41**, 081002 (2008).
- [11] J. Itatani, J. Levesque, D. Zeidler, H. Niikura, H. Pepen, J. C. Kieffer, P. B. Corkum, and D. M. Villeneuve, *Nature (London)* **432**, 867 (2004).
- [12] V. H. Le, A. T. Le, R. H. Xie, and C. D. Lin, *Phys. Rev. A* **76**, 013414 (2007).
- [13] H. Wabnitz, Y. Mairesse, L. J. Frasinski, M. Stankiewicz, W. Boutu, P. Breger, P. Johnsson, H. Merdji, P. Monchicourt, P. Salieres, K. Varju, M. Vitteau, and B. Carre, *Eur. Phys. J. D* **40**, 305 (2006).
- [14] X. Zhou, R. Lock, W. Li, N. Wagner, M. Murnane, and H. Kapteyn, *Phys. Rev. Lett.* **100**, 073902 (2008).
- [15] N. Wagner, X. Zhou, R. Lock, W. Li, A. Wuest, M. Murnane, and H. Kapteyn, *Phys. Rev. A* **76**, 061403(R) (2007).
- [16] T. Kanai, E. J. Takahashi, Y. Nabekawa, and K. Midorikawa, *Phys. Rev. A* **77**, 041402(R) (2008).
- [17] T. Kanai, E. J. Takahashi, Y. Nabekawa, and K. Midorikawa, *Phys. Rev. Lett.* **98**, 153904 (2007).
- [18] J. Levesque, D. Zeidler, J. P. Marangos, P. B. Corkum, and D. M. Villeneuve, *Phys. Rev. Lett.* **98**, 183903 (2007).
- [19] Z. Chen, T. Morishita, A. T. Le, M. Wickenhauser, X. M. Tong, and C. D. Lin, *Phys. Rev. A* **74**, 053405 (2006).
- [20] A. F. Starace, *Theory of Atomic Photoionization* (Springer-Verlag, Berlin, 1982), p. 14.
- [21] C. D. Lin, *Phys. Rev. A* **9**, 181 (1974).
- [22] M. Ya. Amusia, N. A. Cherepkov, and L. V. Chernysheva, *Sov. Phys. JETP* **33**, 90 (1971).

- [23] M. Yu. Ivanov, T. Brabec, and N. Burnett, *Phys. Rev. A* **54**, 742 (1996).
- [24] O. Smirnova, M. Spanner, and M. Ivanov, *J. Phys. B* **39**, S307 (2006).
- [25] J. Z. Kaminski and F. Ehlotzky, *Phys. Rev. A* **54**, 3678 (1996).
- [26] T. Kanai, S. Minemoto, and H. Sakai, *Nature (London)* **435**, 470 (2005).
- [27] C. Vozzi, F. Calegari, E. Benedetti, J.-P. Caumes, G. Sansone, S. Stagira, M. Nisoli, R. Torres, E. Heesel, N. Kajumba, J. P. Marangos, C. Altucci, and R. Velotta, *Phys. Rev. Lett.* **95**, 153902 (2005).
- [28] A. T. Le, X. M. Tong, and C. D. Lin, *Phys. Rev. A* **73**, 041402(R) (2006).